PRAMANA
— journal of
physics

Vol. 80, No. 6
June 2013
pp. 1065–1081

Durability of rewritable phase-change $Ge_XSb_YTe_{1-X-Y}$ memory devices

N PARVATHALA REDDY[1], CH BAPANAYYA[2], RAJEEV GUPTA[1,2] and S C AGARWAL[1,*]

[1]Department of Physics; [2]Materials Science Programme, Indian Institute of Technology Kanpur, Kanpur 208 016, India

*Corresponding author. E-mail: sca@iitk.ac.in

MS received 6 October 2012; accepted 22 January 2013

Abstract. The bond constraint theory (BCT) dealing with the rigidity caused by bond constraints and the long-range potential fluctuations (LRPF) arising from the defects and heterogeneities in the disordered semiconductors are important for understanding the atomic and electronic properties of amorphous semiconductors. Here, they are applied to the already commercialized $Ge_XSb_YTe_{1-X-Y}$ (GST) chalcogenide glasses used in the rewritable phase change memory (PCM) devices. The main concern at present is to improve their ability to withstand a large number of phase change cycles, by choosing the right composition. The two considerations (BCT and LRPF) are briefly described and tested on the most commonly used $Ge_2Sb_2Te_5$ and the nearby compositions. While these considerations provide significant insight into their atomic and electronic structures, the ansatz linking them with the durability of the PCM devices need to be justified by more work.

Keywords. Chalcogenide glasses; extended X-ray absorption fine structure; bond constraint theory; thermopower; long-range potential fluctuations

PACS Nos 78.66.Jg; 61.43.Dq; 61.43.Fs

1. Introduction

The chalcogenide glasses have been paid considerable attention since the discovery [1] of switching and memory effects in them. The structural, optical and electrical properties of chalcogenides have been studied and several novel effects have been discovered. The observation of giant photocontraction in the obliquely deposited thin films of GeSe by Chopra *et al* [2] is an example. The ability of chalocogenides to transform quickly and repeatedly between the amorphous and crystalline states is very useful for nonvolatile rewritable recording. Today, the phase change memory (PCM) is a promising candidate for the future memory technology [3]. Among the Ge–Sb–Te alloys, the performance of $Ge_2Sb_2Te_5$ (hereafter GST 225) is outstanding [4–6], in terms of speed, stability, and

endurance. This alloy is already being used in optical memory devices like RW-DVD/CD, PRAM etc. It crystallizes in a very short period of time (typically 20 ns), at its crystallization temperature (150°C). It can also withstand $\sim 10^{12}$ cycles before failing [3], which is relatively high among chalcogenide glasses, the highest reported for a particular set of set/reset pulses. This, however, needs to be increased by several orders of magnitudes, before it can be used as system memory, in a computer [7], for example.

Thus, two main issues are to be addressed in materials for the rewritable PCM devices. First is the identification of suitable materials with the following requirements: Their amorphous and crystalline states should be stable and yet it should be possible to go very quickly from one state to the other. Further, they must have at least one significantly different property (e.g. reflectivity) in the two states, which can be used as a memory code. The second issue has to do with the durability of device, i.e. the number of cycles the device can withstand before failing. While the first issue has been tackled more or less successfully by several authors, the same cannot be said about the second.

Efforts to find new compositions for the memory devices to increase their durability have so far been largely based on trial and error. This may be partly, because of the inadequate understanding of the phase change phenomena, resulting in the non-availability of a suitable way to identify, *a priori*, new and better PCM materials. Several scientists [8,9] have tried to elucidate the structural changes that might give widely different properties, but most of them did not address the problem of durability. For example, Shportko *et al* [10] suggested measurement of electronic polarizability as a simple test to identify potential phase change materials, having 70 to 200% larger optical dielectric constant in the crystalline phase than in the amorphous phase. However, the durability was not discussed. Kolobov *et al* [9] have proposed an interesting model to explain the phase change process in GST 225. According to them this transition involves the so-called umbrella-flip of Ge atoms from an octahedral position to a tetrahedral position without breaking strong covalent bonds. This flip-flop gives GST 225 the ability to switch between the two states, many more times than the other glasses. However, the proposed model completely ignored Ge–Ge bonds in the amorphous state. These bonds, according to bond constraint theory (BCT), can help explain the excellent behaviour of GST 225. Moreover, the presence of homopolar Ge–Ge bonds is consistent with extended X-ray absorption fine structure (EXAFS) measurements and their new analysis [11]. In any case, while the Kolobov's model [9] might explain the relatively better durability of GST 225, it did not tell us how to select another composition in order to improve it. In another model [12], it was argued that the intrinsic vacancies present in the metastable crystalline cubic phase are ordered in (1 1 1) planes. These vacancies help the movement of Ge atoms from octahedral coordination in the crystalline (cubic) phase to tetrahedral coordination in the amorphous phase. The high endurance is achieved by the optimal combination of intrinsic vacancies provided by Sb_2Te_3 and the instability of the tetrahedron sites provided by GeTe. Recently, Siegrist *et al* [13] proposed that the phase change materials have a pronounced disorder but a weak electron correlation, making them an 'unparalleled quantum state of matter'. An Anderson-type metal–insulator transition occurs upon increasing the temperature because of strong disorder. This explains the high ratio of resistivities of the crystalline and amorphous states in GST 225. However, regardless of whether any of these or the other proposed models is true, they do not provide an easy way to look for and identify, *a priori*, sturdier materials for use in the PCM devices.

Basically, two ideas have been put forward to tackle the durability issue. One of them uses bond constraint theory (BCT) [11,14,15] and the other considers the long-range potential fluctuations (LRPF) in the amorphous state [16,17] to estimate the durability.

The next section briefly describes the BCT, defines an ideal glass former and shows how the presence of Ge–Ge bonds in GST 225 makes it a good glass former. Section 3 gives experimental details for investigating long-range potential fluctuations, caused by the Te_3^+ ions and the other defects, by transport measurements. The last two sections discuss the results and arrive at conclusions.

2. Bond constraint theory (BCT)

Here, the general physical ansatz is that in an ideal, strain-free thin film or bulk amorphous material, the number of constraints equals the number of degrees of freedom in space (or network dimensionality). This means that the ideal material has just the right number of constraints to be neither floppy nor overconstrained. Since the thin film materials in this article are three-dimensional, the average number of constraints/atom, $C_{\rm av}$, for an ideal material is given by

$$C_{\rm av} = 3. \tag{1}$$

Thus, according to BCT, a material with a smaller deviation from the ideal value $\delta C_{\rm av} = |C_{\rm av} - 3|$ is likely to be a 'better glass-former' which means that its ability to transform itself from one phase to the other easily and repeatedly is superior. This criterion can be useful for identifying durable materials for memory applications.

We shall now calculate $C_{\rm av}$ for GST 225, using BCT along with the input from EXAFS experiments [11] and show that GST 225 satisfies the criterion of eq. (1) better, if it has Ge–Ge bonds.

According to BCT, $C_{\rm av}$ is related to the average coordination number $\langle r \rangle$ as follows [18]:

$$C_{\rm av} = \frac{5\langle r \rangle}{2} - 3. \tag{2}$$

In order to calculate $C_{\rm av}$ for GST 225, we must know its bonding structure. The Te–Sb–Ge ternary phase diagram in figure 1 provides a basis for understanding the structure and properties of GST. The GST 225 compound lies at the intersection of two lines of interest: a tie-line joining GeTe and Sb_2Te_3; and the bisector of the angle at the Te vertex. Thus, one might conclude that GST 225 is a mixture of GeTe and Sb_2Te_3. However, there is another possibility, which is physically even more interesting. Here, GST 225 is supposedly on the tie-line joining two potentially good glass-forming compositions: Ge_2Te_3 and Sb_2Te_3. Therefore, rather than considering it to be an equal mixture of 2(GeTe) and Sb_2Te_3, one can view it as a Te deficient mixture of Ge_2Te_3 and Sb_2Te_3 in a matrix of cross-linked two- and three-fold coordinated Te atoms.

Let us look at the experimental evidence to find out on which of the two tie-lines, viz. {Ge_2Te_3–Sb_2Te_3} or {GeTe–Sb_2Te_3}, GST 225 should lie, to be consistent with being a good glass former.

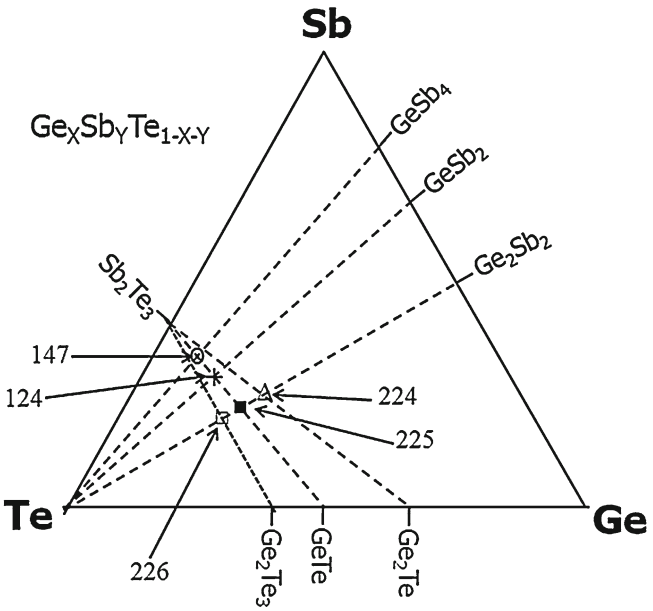

Figure 1. Ternary phase diagram for Ge–Sb–Te compounds, showing locations of compounds considered in this article, and the various tie-lines.

Coordination numbers N for the constituent atoms of GST 225, as determined from EXAFS, indicate fully coordinated Ge and Sb with $N_{\mathrm{Ge}} = 3.9 \pm 0.7$ and $N_{\mathrm{Sb}} = 2.8 \pm 0.5$ and slightly overcoordinated Te with $N_{\mathrm{Te}} = 2.4 \pm 0.6$ [19].

EXAFS technique also shows that the only homopolar bonds are Ge–Ge bonds, and approximately 1/7 (or ∼14%) of the Ge bonds are homopolar. The presence of homopolar bonding of Ge suggests a model where all Ge atoms are bonded to one Ge and three Te atoms in a-Ge_2Se_3-type bonding [20] as shown in figure 2. Sb atoms are then interspersed evenly throughout the structure with three Te neighbours in Sb_2Te_3 arrangements. The molecular structure of GST 225 thus includes the following local bonding arrangements: (i) Sb_2Te_3, (ii) Ge_2Te_3, and (iii) three-fold coordinated Te atoms, the nearest neighbours of which are Sb and Ge.

We can now calculate C_{av} for GST 225 for the two cases: (I) Without homopolar Ge–Ge bonds and (II) with homopolar Ge–Ge bonds.

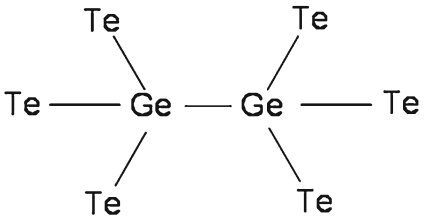

Figure 2. Ge_2Te_3 configuration, as might be present in $Ge_2Sb_2Te_5$ (after ref. [19]).

Case I: $Ge_2Sb_2Te_5$ is on the {GeTe–Sb_2Te_3} tie-line and has no Ge–Ge bonds.

$$\begin{aligned} \text{For Ge: } \langle r\rangle &= 4 \quad C_{\text{Ge}} = 7, \\ \text{Sb: } \langle r\rangle &= 3 \quad C_{\text{Sb}} = 4.5, \\ \text{Te: } \langle r\rangle &= 2 \quad C_{\text{Te}} = 2. \end{aligned}$$

Therefore, for $Ge_2Sb_2Te_5$,

$$C_{\text{av}} = (7\times 2 + 4.5\times 2 + 2\times 5)/9 = 3.66 \text{ and } \delta C_{\text{av}} = 0.66. \tag{3}$$

Case II: $Ge_2Sb_2Te_5$ is on the {Ge_2Sb_3–Sb_2Te_3} tie-line and has Ge–Ge bonds.

Consider first the local bonding environment for Ge. To zeroth order, a tetrahedral Ge configuration yields $C_{\text{Ge}} = 7$, as in Case I. However, the presence of homopolar Ge–Ge bonds has a profound effect on constraint counting. Assuming that all Ge atoms are bonded as shown in figure 2, the bending constraints around each Ge are (i) Ge–Ge–Te and (ii) Te–Ge–Te motions. The motion of Ge–Ge–Te is much smaller than Te–Ge–Te, because they have different bond energies, permitting removal of some constraints. This and other similar considerations [6] reduce the total number of constraints for Ge atoms from $C_{\text{Ge}} = 7$ to 4.33.

In the Sb bonding environment, we find that none of the constraints are broken. Therefore, the total number of constraints around the Sb atoms is $C_{\text{Sb}} = 4.5$.

Finally, consider the Te bonding environment. In the proposed model, GST is a combination of Ge_2Te_3 and Sb_2Te_3 structural units. This counting results in a deficiency in Te for the GST composition, as stoichiometry requires that the addition of these two units equals $Ge_2Sb_2Te_6$. This means 1/6 (∼17%) Te deficiency, which combined with $8-N$ coordination of Ge and Sb requires that some Te atoms overcoordinate, resulting in the presence of both two- and three-fold geometries. No constraints can be removed for the former configuration, and in the latter, the bond order is reduced from one electron/bond to 2/3 electrons/bond. Constraints are removed for this configuration, but proportionally so [19], resulting in two constraints for planar three-fold coordinated Te, as well as two-fold coordinated Te. Therefore, the number of total constraints for all Te atoms is 2.

The total number of constraints for the GST 225 alloy is then calculated as follows [20]:

Ge contribution: $4.33\times 2 = 8.66$; Sb contribution: $4.5\times 2 = 9$; Te contribution: $2\times 5 = 10$.

Thus,

$$C_{\text{av}} = (8.66 + 9 + 10)/9 = 3.07; \quad \delta C_{\text{av}} = 0.07. \tag{4}$$

This value of δC_{av} is smaller than the value obtained for Case I in eq. (3). As already remarked earlier, we have called it a good glass former, which in the present context means that it can be easily and repeatedly transformed from amorphous to crystalline state and back. Further, it does not refer to the ease of making glass of this composition.

Clearly, the inclusion of Ge–Ge bonds in $Ge_2Sb_2Te_5$ is responsible for giving it good glass forming capability and the propensity for repeatable phase change transitions. It also predicts the presence of defects associated with of three-fold coordinated Te_3^+.

3. Long-range potential fluctuations (LRPF)

Following Overhof and Beyer [21,22], we have used electronic transport measurements [16] to estimate the LRPF caused by Te_3^+ and other defects. The GST alloy compositions chosen are GST 224, 225, 226, 124, and 147. The alloys GST 124 and GST 147 lie on $GeTe–Sb_2Te_3$ tie-line [4] in the Ge–Sb–Te phase diagram (figure 1). GST 224 and 226 lie very close to GST 225 and are on different tie-lines. While GST 226 lies on $Ge_2Te_3–Sb_2Te_3$ tie-line, GST 225 and GST 224 can be considered to be on this line, with Te deficiency. The idea behind the selection is to compare the change in potential fluctuations in GST 225 (which shows the best performance including endurance), with nearby compositions. Our experiments and results are described below.

3.1 *Experimental details*

GST chalcogenide alloys were prepared in bulk by melt quenching the appropriate quantities of the desired constituents and were ground to powder form. Thin films were deposited in vacuum (1×10^{-5} Torr) onto Corning 7059 glass, using a flash evaporator described elsewhere [23]. The prepared GST powder was allowed to fall slowly from a hopper onto a tungsten boat kept at ≈1000°C. No external heating of substrates was done. Films of thicknesses ranging between 500 and 800 nm were deposited at the rate of ∼10 nm/s. The compositions of the films were checked using energy-dispersive X-ray (EDX) analysis and were found to be within 3 at% of the starting compositions [23].

For electrical measurements, two parallel strips of nichrome electrodes separated by 3 mm were vacuum evaporated on the films in a coplanar geometry. The as-deposited films were found to be ohmic up to the highest field (330 V/cm). Crystalline films were obtained by annealing the amorphous samples at 200°C for 30 min in vacuum (1×10^{-5} Torr). Further, a GST 225 sample was re-amorphized by exposure to one pulse (270 mJ, 20 ns) from an excimer laser (wavelength = 248 nm) operating at 1 Hz and was re-measured to check the reproducibility. This was crystallized once again by annealing as before and then measured again in this state.

The system was stabilized at the desired temperature T and the thermopower $S(T)$ and conductivity $\sigma(T)$ were measured simultaneously, at each T (300 K $\leq T \leq$ 420 K). Two separate heaters were used to individually control the temperature of the two ends of the sample and the temperature was monitored using two copper–constantan thermocouples mounted at each end (which were also the electrodes). The difference of temperature (ΔT) between the two ends of the sample was measured by shorting the constantan wires of the thermocouples and measuring the thermo emf across the copper leads. Care was taken to choose a pair of thermocouples, which were matched to give $\Delta V = 0$, for $\Delta T = 0$, in the entire range of T. The temperature difference (ΔT) was varied between 0 and 5 K and the thermoelectric voltage (ΔV) was measured across the copper wires of the thermocouple with constantan wires disconnected. The slope of the straight line in the ΔV vs. ΔT plot at each T gives the thermopower (S). At high resistance values, the sample can pick up a lot of noise and to avoid it, the chamber and the thermocouple wires coming out of the chamber were properly shielded. All measurements were done in a thermally conducting inert gas atmosphere (helium at ∼2 Torr) to ensure good

thermal contact between the sample and the thermocouples. Details of the measurement apparatus are given in ref. [24].

3.2 *Results and discussion*

The temperature dependence of conductivity of the various compositions of the as-deposited samples is shown in figure 3. All five compositions exhibit Arrhenius behaviour:

$$\sigma(T) = \sigma_0 \exp(-E_\sigma^*/k_B T), \tag{5}$$

where σ_0 is the conductivity prefactor, E_σ^* is the measured activation energy and k_B is the Boltzmann constant. The error bars are about the size of the data points. The activation energies (E_σ^*) are summarized in table 1. The conductivity data of GST 225 is in agreement with data in refs [25–27].

Figure 4 shows the thermoelectric power $S(T)$ of the as-deposited samples plotted as a function of reciprocal temperature. All samples show positive thermopower and hence the majority charge carriers are holes, which is the case for most of the chalcogenide glasses [26,28]; $S(T)$ seems to follow the relation:

$$S = \left(\frac{k_B}{e}\right)\left(\frac{E_S^*}{k_B T} + A\right), \tag{6}$$

where E_S^* is the measured slope of the thermoelectric power, e is the absolute value of electronic charge and A is the heat of transport term ($A \approx 1$) [28]. The slopes (E_S^*) are tabulated in table 1.

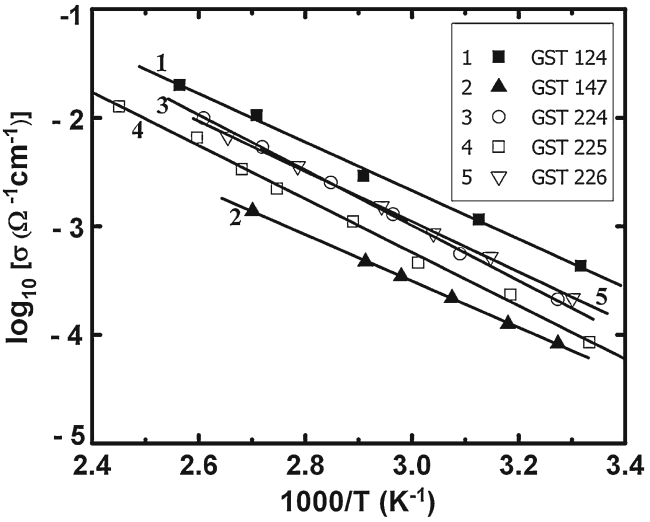

Figure 3. Conductivity as a function of inverse temperature of amorphous GST films. Here GST 124 corresponds to $Ge_1Sb_2Te_4$ and so on. The activation energies (E_σ^*) are given in table 1 (after [16]).

Table 1. Activation energies and widths of potential fluctuations as measured in the thin films of various GST alloys in amorphous and crystalline states.

Alloy	Phase	E_σ^* (eV)	E_S^* (eV)	E_Q (eV)	Δ (eV)
GST 124	Amorphous	0.441±0.015	0.212±0.008	0.229±0.023	0.183±0.018
	Crystalline	0.023±0.001	0.021±0.001	0.002±0.002	0.002±0.001
GST 147	Amorphous	0.422±0.004	0.180±0.003	0.252±0.007	0.202±0.006
	Crystalline		Metallic		
GST 224	Amorphous	0.503±0.007	0.302±0.007	0.201±0.014	0.161±0.011
	Crystalline		Metallic		
GST 225	Amorphous	0.491±0.012	0.350±0.011	0.141±0.023	0.113±0.018
	Crystallized	0.084±0.001	0.081±0.002	0.003±0.003	0.002±0.002
	Re-amorphized	0.412±0.01	0.273±0.004	0.139±0.014	0.111±0.012
	Re-crystallized	0.082±0.001	0.080±0.002	0.002±0.003	0.002±0.002
GST 226	Amorphous	0.464±0.007	0.233±0.009	0.231±0.016	0.185±0.012
	Crystalline	0.041±0.001	0.040±0.005	0.001±0.006	0.001±0.005

We see that $E_\sigma^* \neq E_S^*$, which is found quite often in amorphous semiconductors.

Here, it may be noted that E_σ^* and E_S^* are the measured slopes and their values may be different from the actual separation between the Fermi level and the conducting level, because of the possible statistical shift of the Fermi level E_F, with temperature. This shift of E_F may not show up as a departure from the Arrhenius behaviour, especially if it is linear in T. In view of this uncertainty, Overhof and Beyer [21,22] defined a function $Q(T)$ in which $\sigma(T)$ and $S(T)$ are combined in such a way that Q is independent of E_F.

$$Q(T) = \ln \sigma(T) + (e/k_B)S(T). \tag{7}$$

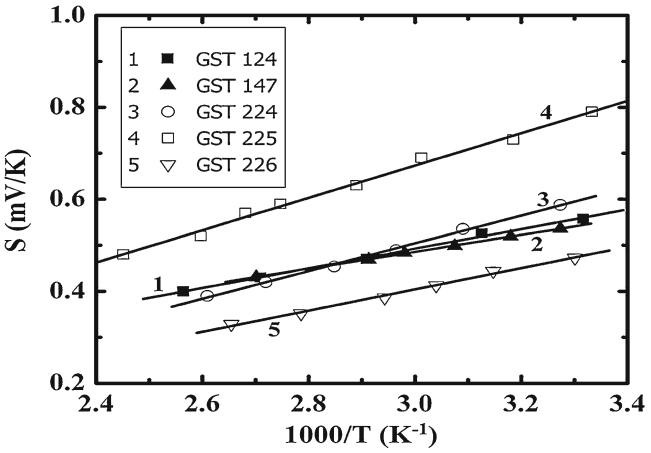

Figure 4. Variation of thermopower of GST alloys as a function of inverse temperature. The slopes (E_S^*) are listed in table 1 (after [16]).

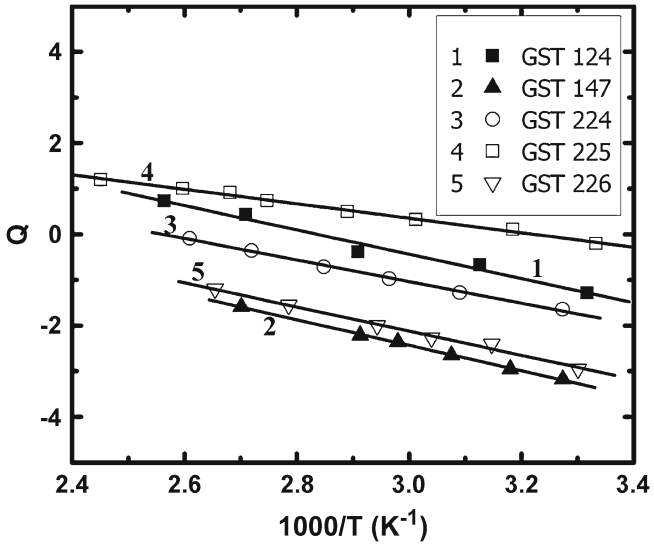

Figure 5. Variation of Q as a function of inverse temperature of amorphous GST samples. Q is defined in eq. (7), so that it is independent of the position of Fermi level (after [16]).

Figure 5 shows $Q(T)$ as a function of inverse temperature. The temperature variation of Q for all samples can be well represented by the following relation:

$$Q(T) = Q_0 - \frac{E_Q}{k_B T} \tag{8}$$

with $Q_0 = \ln \sigma_0 + A$ and $E_Q = E^*_\sigma - E^*_S$. That is, the slope E_Q of Q is a measure of discrepancy between the slopes of $\sigma(T)$ and $S(T)$.

Overhof and Beyer [21,22] have suggested that the presence of long-range potential fluctuations might be a likely cause of the difference between E^*_σ and E^*_S.

The charged centres in GST create long-range static potential that modulates the conduction as well as valence band edges equally in the same direction [28,29] (see figure 6a).

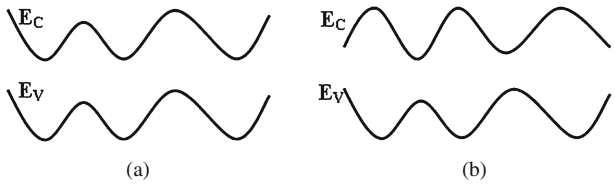

Figure 6. Band edge fluctuations in amorphous semiconductors (a) symmetric (b) antisymmetric.

This modulation gives rise to fluctuations in mobility edges, which are known as 'long-range potential fluctuations' (LRPF). The range of these potential fluctuations is assumed to be large enough ($l \sim$10 nm) to disallow tunnelling and strong localization.

In hydrogenated amorphous silicon, Overhof and Beyer [22] assumed a non-homogeneous distribution of charged centres throughout the sample. They divided the sample into cubes of length l and assumed that the mobility edge has a constant value in each cube. Further, a Gaussian probability distribution function of width Δ was used to assign the position of mobility edge in each cell. Using a computer, Overhof and Beyer obtained for concentration N_c of charged defects, an empirical relationship between the width of potential fluctuations (Δ) and the difference (E_Q) between the measured activation energies of conductivity and thermopower [22].

$$E_Q = E_\sigma^* - E_S^* = 1.25\Delta. \tag{9}$$

Further, it can be shown [22] that for a concentration N_c of charged defects:

$$E_Q = \alpha\sqrt{N_c}, \tag{10}$$

where α is a constant that depends on the macroscopic properties such as dielectric constant and refractive index of the material. For small variations in composition, α is not likely to vary much, from sample to sample. Hence, samples with higher concentration of charged centres (N_c) are expected to have a higher width of potential fluctuations (Δ), if α does not vary much, from sample to sample.

Although relations (5) and (6) were initially obtained for a-Si:H, they are likely to hold for chalcogenide glasses as well [30]. Here, the role of charged defects in doped a-Si:H might as well be played by Te_3^+. In chalcogenide glasses, the lowest energy defects are not the neutral dangling bonds, but the charged centres associated with over- or undercoordinated atoms. That is why the chalcogenide glasses do not show ESR [31], as explained by Kastner *et al* [32]. They do not have dangling bonds because they have a lone (non-bonding) pair of electrons, which can provide or accommodate additional electrons in the case of over- or undercoordination. These charged defects are expected to cost less energy than the dangling bonds. Since the material on the whole is neutral, these defects appear in pairs of positive and negative charges, known as valance alternation pairs (VAPs) [32]. In the present case, these might be Te_3^+ and Sb^- [19]. The majority of these will be near each other as pairs because of electrostatic attraction. They will form the so-called electrostatic bond and therefore, may not contribute to LRPF. However, there will be some that will be far enough to produce LRPF. As already mentioned above, the presence of three-fold coordinated tellurium in amorphous GST 225 is envisaged using BCT and is supported by experimental results of EXAFS.

The temperature dependence of conductivity, thermoelectric power and $Q(T)$ of crystalline films (shown only for GST 225 in figures 7 and 8) are qualitatively similar to the amorphous ones for almost all compositions. However, their magnitudes and activation energies are quite different (table 1). Further, Q varies very little as a function of temperature, giving a zero slope (E_Q). Table 1 summarizes the values of E_Q and other important quantities. GST 224 shows a metallic behaviour in the crystalline state and therefore its slopes etc. are not given in the table.

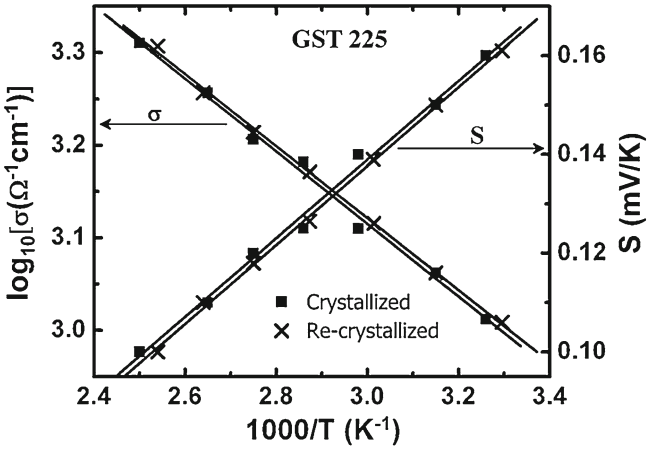

Figure 7. Log conductivity (σ) and thermopower (S) of crystallized and re-crystallized GST 225 as a function of inverse temperature (please note the two ordinate scales for σ and S). The data are essentially unchanged after re-crystallization [17].

We assume the charged defects in the chalcogenide glasses to be uniformly distributed, as done by Overhof and Beyer [22] in the case of a-Si:H. Figure 9 shows the values of Δ calculated using eq. (9) for various GST compositions in amorphous and crystalline states. The width changes from a nonzero value in the amorphous state to zero in crystalline state. The change in Δ upon phase change is therefore, Δ itself. Δ varies between 0.113 ± 0.018 eV and 0.202 ± 0.006 eV, for different compositions, and is the smallest for GST 225 (0.113 ± 0.018 eV). A small change in tellurium concentration from GST 225 leads to a larger Δ for GST 224 and GST 226. Further, the compositions GST 124 and

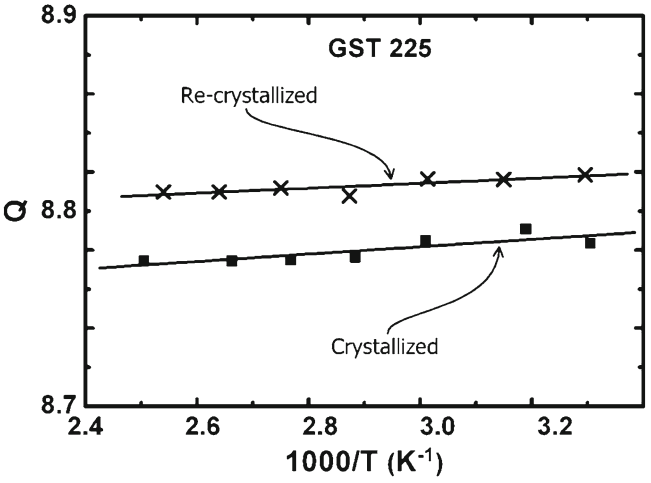

Figure 8. Q as a function of inverse temperature for crystallized and re-crystallized GST 225. Please note the reproducibility of the slope.

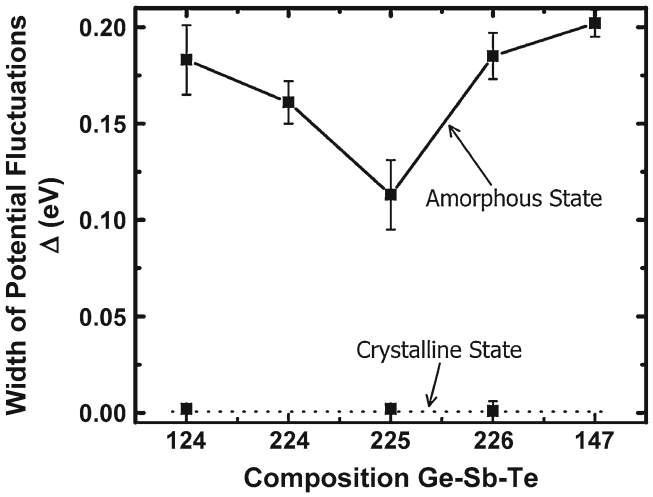

Figure 9. Widths of potential fluctuations (Δ) calculated and tabulated (table 1) for GST samples in amorphous and crystalline phases. The GST 225 film shows the smallest potential fluctuations compared to the other compositions. Note that Δ in crystalline phase is zero [17].

GST 147 also show a larger Δ. The error bars shown arise mainly from the deviation from the straight line fit to the data. To verify these ideas, we re-amorphized the GST 225 film, by exposing it to a pulse of UV light from an Excimer laser (described in §3.1). As shown in figure 10, the conductivity of the re-amorphized sample is a bit higher and thermopower slightly lower than that of the as-deposited film. But, using the thermopower

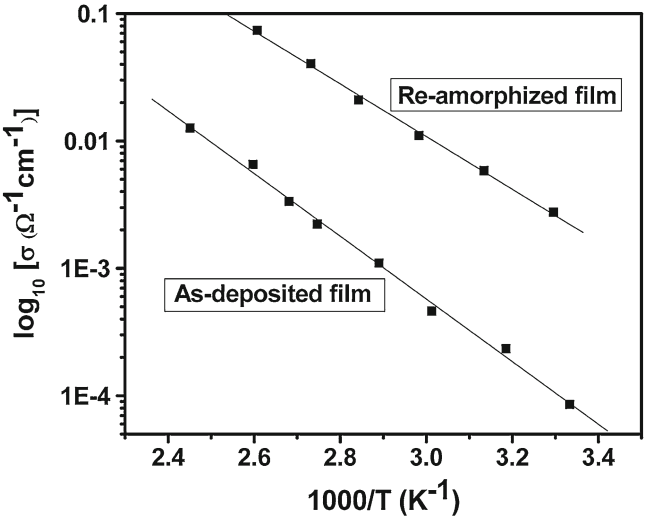

Figure 10. Conductivity $\sigma(T)$ data of an 'as-deposited' amorphous GST 225 film compared with the re-amorphized GST 225 film.

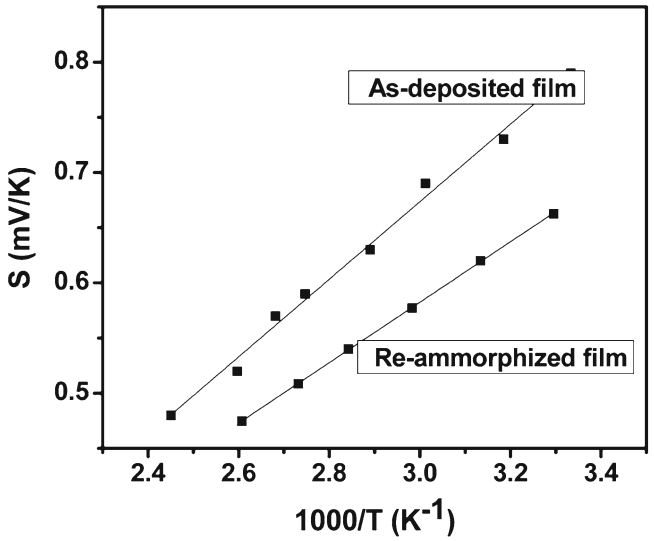

Figure 11. Comparison of thermopower $S(T)$ of a GST 225 film in the 'as-deposited' and re-amorphized states.

data in figure 11, we find that the slope E_Q in figure 12 is unchanged (within error bars) after re-amorphization. Further, in the re-crystallized state, $\sigma(T)$ and $S(T)$ are not very different compared to the first cycle (figures 7 and 8). Therefore, the widths of potential fluctuations in the as-deposited GST 225 and in re-amorphized one are within the error

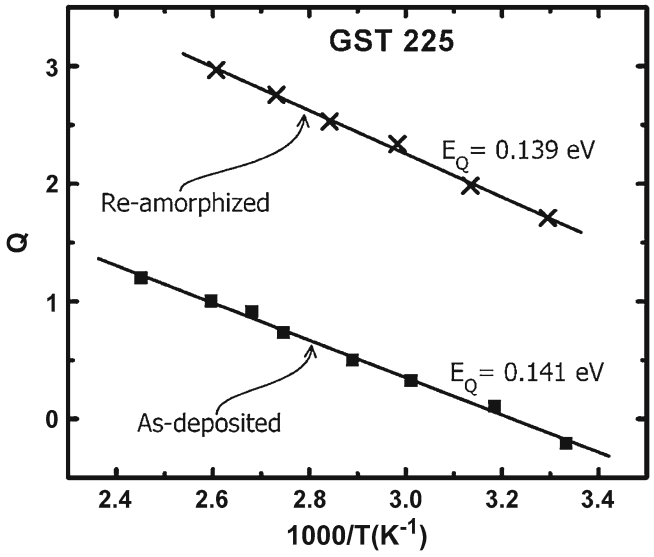

Figure 12. Comparison of Q of an as-deposited GST 225 film and re-amorphized film as a function of inverse temperature T. Please note that although $\sigma(T)$ and $S(T)$ change after re-amorphization (figures 10 and 11), $Q(T)$ remains unchanged [17].

bars of each other. Furthermore, there is no change in the slopes E_σ, E_S and E_Q (table 1) after re-crystallization.

As noted earlier, GST 225 is known to be [3] one of the best phase change materials which can undergo quite a large number of write-erase cycles fairly quickly. This excellent behaviour may be related to the very small E_Q in the amorphous state. Indeed, we note that the other less efficient materials exhibit higher values of E_Q. As per eq. (10), a smaller value of Δ in amorphous phase indicates lower concentration of charged defects, i.e., VAPs. Hence the structure of amorphous GST 225 may be regarded as less disordered compared to the other compositions. So, in going from amorphous to crystalline phase (ordered), GST 225 is required to undergo fewer structural changes compared to the other alloys. A material which, upon phase change undergoes minimal structural changes, is more likely to have a longer life.

Hence, a material with fewer defects and therefore smaller Δ is to be preferred for use in PCM devices. This material must, of course, have stable amorphous and crystalline states and should have sufficiently different physical properties in the two states. Further study on other materials is necessary to strengthen these views.

4. Analysis

According to BCT, the material for which the number of bond constraints is closer to 3 (eq. (1)), is expected to perform better, as this makes the material neither overconstrained nor floppy; ideal for going from amorphous to crystalline state and back, many times. We have called it a good glass former.

We have seen that GST 225 will satisfy the BCT requirement, i.e. eq. (1), if it has homopolar Ge–Ge bonds and as a consequence Te_3^+ defects. Let us also check the prediction of BCT criterion for the other GST compositions also (which were chosen for LRPF measurement).

EXAFS data [11,19] on GST 224 and GST 226 suggest that they lie on Ge_2Te_3–Sb_2Te_3 tie-line with GST 224 deficient in Te. While no EXAFS data exist for GST 124 and GST 147, they seem to be on GeTe–Sb_2Te_3 tie-line. The average number of constraints for each alloy is calculated as given below.

$$C_{\text{av}}(224) = [2(4.33) + 2(4.5) + 4(2)]/8 = 3.21,$$
$$(Ge_2Te_3\text{–}Sb_2Te_3 \text{ tie-line}), \quad \delta C = 0.21$$

$$C_{\text{av}}(226) = [2(4.33) + 2(4.5) + 6(2)]/10 = 2.97,$$
$$(Ge_2Te_3\text{–}Sb_2Te_3 \text{ tie-line}), \quad \delta C = 0.03$$

$$C_{\text{av}}(124) = [1(7) + 2(4.5) + 4(2)]/7 = 3.43,$$
$$(\text{GeTe–}Sb_2Te_3 \text{ tie-line}), \quad \delta C = 0.43$$

$$C_{\text{av}}(147) = [1(7) + 4(4.5) + 7(2)]/12 = 3.25,$$
$$(\text{GeTe–}Sb_2Te_3 \text{ tie-line}), \quad \delta C = 0.25.$$

Comparison of these alloys with GST 225 [$C_{av}(225) = 3.07$ and $\delta C = 0.07$], shows that BCT conjecture favours both GST 225 and GST 226, almost equally.

On the other hand, the LRPF considerations in §3.2 suggest that the material with the smallest Δ should be the best. As Δ for GST 225 is smaller than for the rest of the compositions studied (figure 9), GST 225 is the most suitable. Since the other compositions including GST 226 have actually not been found as useful as GST 225, it seems that the measurement of potential fluctuations is a better indicator of a good glass former. However, question now arises about how GST 225 can have fewer defects (Te_3^+) than GST 226, since GST 225 is Te deficient whereas GST 226 is not. The answer may be that Te_3^+ defects are not the only charged defects that give rise to LRPF. Further, the heterogeneities in the material caused by local structural and compositional variations within the sample also contribute to the LRPF. In the case of charged defects the LRPF are correlated, i.e., the conduction and valance band mobility edges change in phase (figure 6a). But, in the case of heterogeneities, they are uncorrelated as the local band gap may vary from place to place. This can give rise to a potential in which the two edges may shift in opposite directions (figure 6b). Overhof and Beyer [22] have reported that the procedure used for obtaining the relation between E_Q and Δ (similar to eq. (9)) for uncorrelated LRPF arising from the heterogeneities, yields unphysically large values of Δ, provided LRPF alone are assumed to be responsible for the observed E_Q. While it has not been possible to separate the two contributions, it appears reasonable to say that the measured E_Q has in it the contribution from both types of LRPF, and both the charged defects as well as the heterogeneities contribute to Δ. Here, it seems that the total contribution from all sources together happens to be larger for GST 226 than for 225, resulting in a smaller Δ for GST 225.

5. Summary and conclusions

Both BCT and LRPF conjectures give information about the structure of GST 225. BCT ansatz favours the homopolar Ge–Ge bonding and Te deficiency. Also, BCT as well as LRPF lead us to conclude the existence of Te_3^+ and other charged defects and heterogeneities. From the electrical transport properties $\sigma(T)$ and $S(T)$ of GST alloys, the widths of potential fluctuations (Δ) present in various thin films are estimated. The important finding is that the change in Δ upon phase change is the smallest for amorphous GST 225, compared to all other GST alloys studied here. The changes in Δ are expected to be related to structural changes that occur during phase transformations. The material which has a larger change in Δ undergoes larger structural changes upon transformation and hence wears out faster. As Δ for the crystalline state is almost zero, the better material should have a smaller Δ in the amorphous state. This conjecture can serve as a useful criterion to identify compositions that are expected to be suitable for making more durable PCM devices. Furthermore, VAPs (the lowest energy charged defects in chalcogenide glasses) and heterogeneities are identified as the defects that give rise to LRPF. Therefore, it follows that the best switching material should have the smallest density of VAPs and be homogeneous. Although this idea seems reasonable, further work is needed.

These results are compared with the predictions of BCT conjecture which says that the number of constraints for a good glass former should be close to 3. We note that both GST

225 and GST 226 satisfy this criterion equally well. This is at variance with the LRPF prediction and also with the reality, since GST 226 is not known for its good glass forming properties. Thus, it appears that Δ is a better indicator of the suitability of composition than BCT conjecture, at least in this case. However, it is too early to make this statement. We note that Micoulaut *et al* [15] also applied BCT conjecture, but used a different method for counting constraints, using first principles molecular dynamics simulations. It would be interesting to check whether their new procedure can resolve this anomaly.

On the question of GST 225 having Δ smaller than GST 226, even though it is Te deficient (and is therefore expected to have more Te_3^+), we have argued that in addition to the charged Te_3^+ defects, the other defects, and structural and compositional inhomogeneities must also contribute to the potential fluctuations. These (defects, heterogeneities etc.) get frozen in the material as the sample is cooled to below its glass transition temperature (T_g) during preparation. The higher is the T_g, the more will be the frozen-in defects. This suggests that T_g for GST 226 should be higher than that for GST 225. Our attempts to measure T_g did not succeed [33]. It is not easy to measure T_g in thin films of these glasses and so far we have not found any estimate of T_g, in [34], for these glasses.

In the end, it is only fair to point out that both BCT and LRPF tests are based on conjectures. In BCT we consider the bond constraints on the structure and have the ansatz $C_{av} = 3$ for the suitable material. In the second test we consider the heterogeneities and defects that give rise to LRPF. Here the ansatz is that most suitable material will have the smallest Δ. The data are too few at present, to say with any certainty, if either or both of these will solve the problem of searching for durable PCM devices. Testing of these conjectures in different systems and experiments to check their validity, will give the much needed confidence in them.

If they are correct, the best PCM materials should be neither under- nor over-constrained and should be homogeneous and free of defects.

Acknowledgements

The authors are grateful to H Fritzsche, M A Paesler, K L Chopra and P Boolchand for useful comments. The authors also thank R C Budhani for the Excimer laser, and Ram Bilas and the M.Sc. students (M Hemanadhan, Ayoti Patra, Ankit Goel, Ashish Shukla) for help in the experimental work. The financial support by CSIR, New Delhi is also gratefully acknowledged.

References

[1] S R Ovshinsky, *Phys. Rev. Lett.* **21**, 1450 (1968)
E J Evans, J H Helbers and S R Ovshinsky, *J. Non-Cryst. Solids* **2**, 334 (1970)
[2] K L Chopra, K S Harshvardhan, S Rajagopalan and L K Malhotra, *Solid State Commun.* **40**, 387 (1981)
[3] For a comparison of various memory technologies, see, for example, S Natrajan, S Chung, L Paris and A Keshavarzi, *IEEE Solid-State Circuits Mag.* **1**, 34 (2009)
[4] N Yamada, E Ohno, K Nishiuchi, N Akahira and M Takao, *J. Appl. Phys.* **69**, 2849 (1991)
[5] I Friedrich, V Weidenhof, W Njoroge, P Franz and M Wuttig, *J. Appl. Phys.* **87**, 4130 (2000)

[6] S C Agarwal, M A Paesler, D A Baker, P C Taylor, G Lucovsky and A Edwards, *Pramana – J. Phys.* **70**, 245 (2008)
[7] M A Paesler, *The Physics Teacher* **47**, 80 (2009)
[8] W Welnic, A Pamungkas, R Detemple, C Steimer and S Blugel, *Nature Mater.* **5**, 56 (2006)
[9] A V Kolobov, P Fons, A Frenkel, A Ankudinov, J Tominaga and T Uruga, *Nature Mater.* **3**, 703 (2004)
[10] K Shportko, S Kremers, M Woda, D Lencer, J Robertson and M Wuttig, *Nature Mater.* **7**, 653 (2008)
[11] D A Baker, M A Paesler, G Lucovsky, S C Agarwal and P C Taylor, *Phys. Rev. Lett.* **96**, 255501 (2006)
[12] J L F Da Silva, A Walsh, S H Wei and H Lee, *J. Appl. Phys.* **106**, 113509 (2009)
[13] T Siegrist, P Jost, H Volker, M Woda, P Merkelbach, C Schlockermann and M Wuttig, *Nature Mater.* **10**, 202 (2011)
[14] P Boolchand, X Feng and W J Bresser, *J. Non-cryst. Solids* **293–295**, 348 (2001)
[15] M Micoulaut, J-Y Raty, C Otjacques and C Bichara, *Phys. Rev. B* **81**, 174206 (2010)
[16] Ch Bapanayya, Rajeev Gupta and S C Agarwal, *Phil. Mag. Lett.* **91**, 134 (2011)
[17] S C Agarwal, *Phys. Status Solidi B* **249**, 1956 (2012)
[18] J C Phillips, *J. Non-Cryst. Solids* **34**, 153 (1979)
[19] M A Paesler, D A Baker and G Lucovsky, *J. Non Cryst. Solids* **354**, 2706 (2008)
[20] D A Baker, S C Agarwal, G Lucovsky, M A Paesler and P C Taylor, *Mater. Res. Soc. Symp. Proc.* **918**, 157 (2006)
[21] H Overhof and W Beyer, *Phil. Mag. B* **43**, 433 (1981)
[22] H Overhof and W Beyer, *Phil. Mag. B* **47**, 377 (1983)
[23] M Hemanadhan, Ch Bapanayya and S C Agarwal, *J. Vac. Sci. Technol. A* **28**, 625 (2010)
[24] P Agarwal and S C Agarwal, *J. Appl. Phys.* **81**, 3214 (1997)
[25] I Friedrich, V Weidenhof, W Njoroge, P Franz and M Wuttig, *J. Appl. Phys.* **87**, 4130 (2000)
[26] T Kato and K Tanaka, *Jpn. J. Appl. Phys.* **44**, 7340 (2005)
[27] B S Lee, J R Abelson, S G Bishop, D H Kang, B Cheong and Ki-Bum Kim, *J. Appl. Phys.* **97**, 093509 (2005)
[28] N F Mott and E A Davis, *Electronic processes in non-crystalline materials*, 2nd edn (Clarendon Press, Oxford, 1979) p. 235
[29] H Fritzsche, *J. Non-Cryst. Solids* **6**, 49 (1971)
[30] H Overhof and W Beyer, *Phil. Mag. B* **49**, L9 (1984)
[31] S C Agarwal, *Phys. Rev. B* **15**, 685 (1974)
[32] M Kastner, D Adler and H Fritzsche, *Phys. Rev. Lett.* **37**, 1504 (1976)
[33] N P Reddy and S C Agarwal, Unpublished
[34] E M Sanchez, E F Prokhorov, A Mendoza-Galvan and J Gonzalez-Hernandez, *J. Appl. Phys.* **91**, 697 (2002)